World Conference on Timber Engineering Oslo 2023

CYCLIC LOAD TESTS AND NUMERICAL ANALYSIS OF CLT SHEAR WALLS WITH GIR JOINTS

Shuhei Uesugi[1], Daisuke Kadono[2], Katsuhide Murakami[3], Masahide Murakami[4]

ABSTRACT: Four CLT shear wall specimens with GIR joints were subject to cyclic loading. The tensile anchor pre-yielding type specimens exhibited great performance and non-slip response because the M24 ABR steel anchors connected to the GIR joints contributed to resisting in compression. A numerical model using OpenSees was developed to simulate the global response and confirm the energy absorption. A crack was confirmed in one of the specimens before the GIR exhibited its ultimate strength. It is presumed that edge clearance distance may affect CLT shear walls performance for large deformations. The analysis model results are in good agreement with the experimental testing. Finally, the energy absorbed by the tensile bars on the compression side have been quantified.

KEYWORDS: CLT, CLT shear wall, GIR joints, Cyclic load tests, Numerical analysis

1 INTRODUCTION

Cross-laminated timber (CLT) structures have attracted significant attention during the past decade to realise a low-carbon society and carbon sequestration. CLT shear walls are one of the most effective structural systems because of their high strength and in-plane stiffness. CLT shear walls and hybrid structures, such as combined CLT shear walls and steel moment frames have been proposed in the past [1-5]. CLT shear walls are characterised by their rocking behaviour, and the performance of the joints at the ends has a significant impact on the behaviour of the entire CLT shear wall performance [6]. However, it is difficult to realize high-strength and high ductility CLT walls because the strength and ductility of distributed connectors are limited.

In Japan, where earthquakes occur frequently, there is a need for the development of such high-strength and high ductility CLT walls. Aiming at the development of CLT shear walls which final failure properties can ensure high energy absorption properties with stable and ductile failure at the joint, if sufficient tensile performance can be secured using GIR joints that can ensure relatively high bearing capacity, a design method will be similar to reinforced concrete beam members calculation in terms of bending performance.

The authors designed CLT shear walls using GIR joints with high expected strength and confirmed the structure performance by cyclic loading tests. A numerical model is created using OpenSees to simulate the global response and the characteristics of GIR joints are discussed from the viewpoint of energy absorption.

2 SPECIMENS

Figure 1 shows the configuration of Specimen 1 and the steel base. The 0.95 m width and 1.95 m hight CLT shear wall was made of 5-layer, 7-ply cedar S60A CLT panels (@30 × 7 = 210 mm), which were glued with resorcinol adhesive along the width. The strong axis direction of the CLT panels was set in the vertical direction. The GIR joints were filled with epoxy resin adhesive (AICA Kogyo JB-3) and were used for the tensile and shear resisting joints. The anchorage lengths of the tensile and shear rebars were 750 mm and 210 mm, respectively, with D22 bar diameter and rebar grade SD345 which were manufactured by JFE Steel Corporation / Mizutori Works.

Tensile rebars were connected to M24 ABR anchors (manufactured by Dai-rock Ltd.) via mechanical couplers inside the wall base. The yielding capacities of the tensile rebars and ABR anchors were 133.5 kN and 115.0 kN, respectively, and the ABR anchors were expected to yield first. The lower flange of the steel base was tightened by nuts from the upper and lower side. A horizontal stiffener plate was arranged in the middle of flanges to increase the compressive buckling resistance of the M24 ABR anchors. Due to the nuts and the stiffeners, the M24 steel bars are expected to contribute to high energy absorption. Shear rebars were connected to shear plates (PL-12), and the joints between shear bars and shear plates were reinforced by fillet welding. There were long holes along the loading direction at the upper flange of the steel base so as not to the tensile rebars resist to the horizontal force.

Figure 2 shows the arrangement of the GIR joints of each specimen. Specimen 1 had tensile rebars at the second layer from the outside. Specimen 2 had two tensile rebars

[1] Shuhei Uesugi, Nikken Sekkei Ltd., Japan, uesugi.shuhei@nikken.jp
[2] Daisuke Kadono, Nikken Sekkei Ltd., Japan, kadono.daisuke@nikken.jp
[3] Katsuhide Murakami, Nikken Sekkei Ltd., Japan, murakamik@nikken.jp
[4] Masahide Murakami, KINDAI Univ. Faculty of Architecture, murakami@arch.kindai.ac.jp

https://doi.org/10.52202/069179-0275

at the fourth layer from the outside. Both specimens have eight shear-resistant rebars in the middle, placed in fiber direction layers and in the middle eight shear-resistant rebars were placed in fiber direction layers. Specimen 3 had no shear bars, and specimen 4 had only two shear bars. Specimens 1 and 2 were intended to check the tensile-yielding-procedures while specimens 3 and 4 were for checking the shear-yielding-procedures.

3 TEST SETUP

As shown in Figure 1, the specimens were placed horizontally to the ground and supported vertically by linear slider that do not constrain horizontal deformation, thus out-of-plane stiffening was not provided. A constant axial force of 246 kN was applied.

Loading was applied by gradually increasing the cyclic inter-story drift from 1/450, 1/300, 1/200, 1/150, 1/100, 1/75, 1/50, 1/40, to 1/30. These cycles were repeated three times for each amplitude up to ±1/30. Loading was

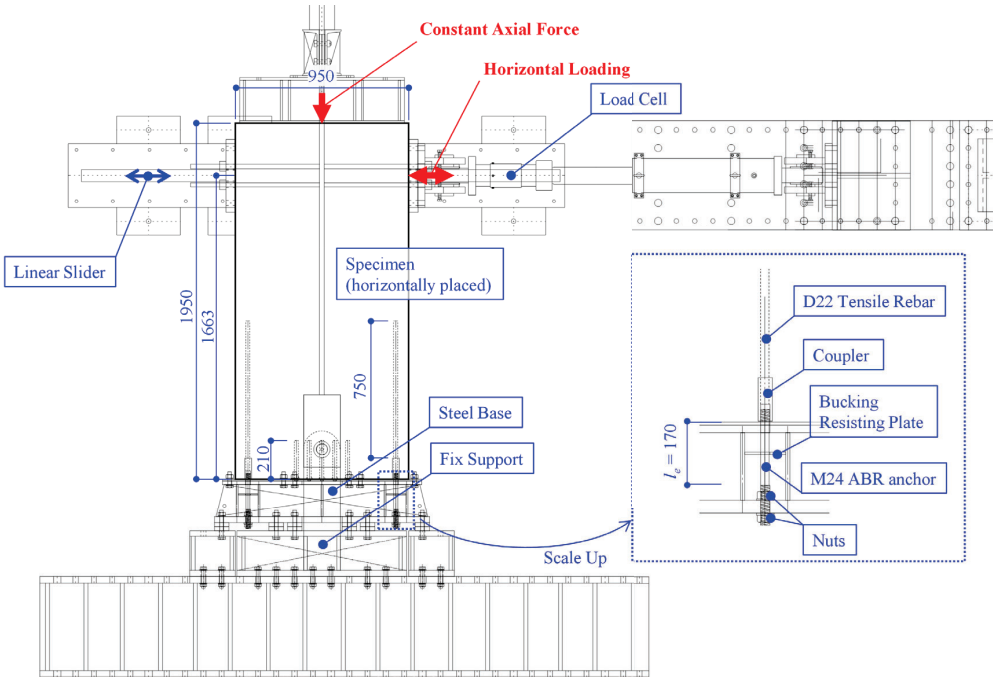

Figure 1: *Configuration of specimen 1 and test setup*

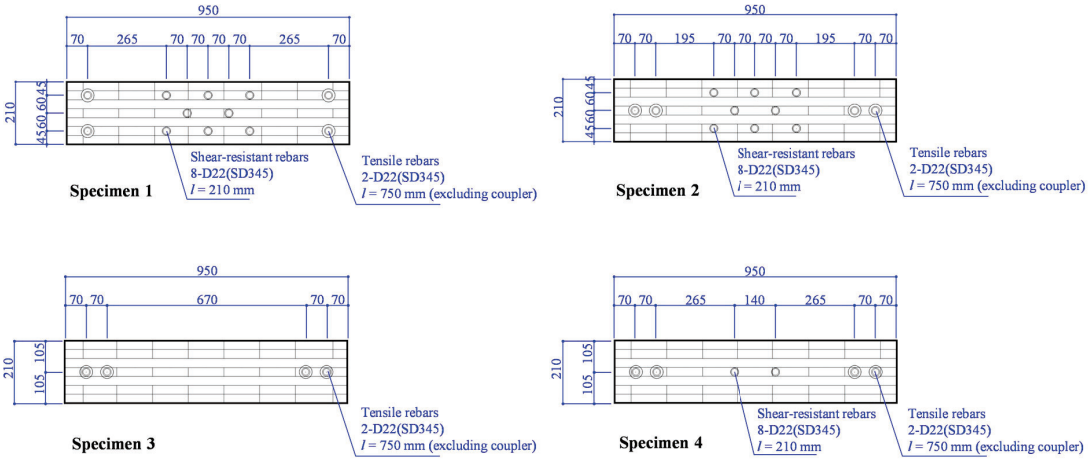

Figure 2: *Arrangement of GIR joints [Unit mm]*

https://doi.org/10.52202/069179-0275

continued until rupture of tensile bars or failure of CLT shear walls was confirmed.

Loading histories for specimen 3 was 1/450 (268kN-3*c*, 402kN-1*c*, 536kN-1*c*), 1/300 (268kN-3*c*, 402kN-1*c*, 536kN-1*c*), 1/100 (268kN-3*c*), 1/75 (402kN-2*c*) and 1/50 (536kN-1*c*). The constant axial force was changed to conform the friction between CLT and steel base and effect of axial force difference. The *c* indicates the number of cycles. In specimen 3, L-shaped steel was installed to restrain horizontal displacement of the CLT shear wall footings at the end of the 1/300 cycle. Figure 3 shows the relationship between shear drift angles and the number of cycles of specimen 3.

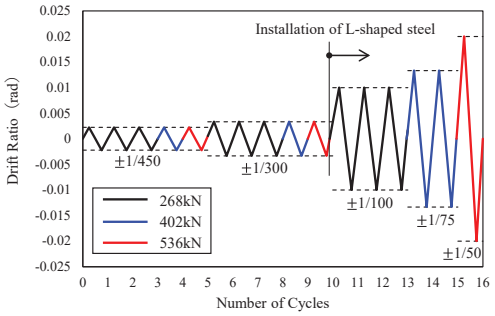

Figure 3: *Loading history at specimen3*

4 TEST RESULTS

4.1 GLOBAL RESPONSE

Figure 4 shows the relationship between horizontal force and horizontal displacement of each specimen (specimen 1 through 4). Specimen 1 exhibited yielding of the tensile rebar during the first excursion up to ±1/100. Subsequently, a stable response was observed up to ±1/75, and CLT cracked at the first excursion up to -1/50. At the second +1/30, the tensile bars were pulled out from CLT, and there was a sudden decrease of the horizontal force. Specimen 2 showed a stable response up to ±1/30, and fracture of the tensile bars was confirmed at a horizontal displacement of about +100 mm. Because tensile bars were arranged inside for specimen 2, the maximum strength of specimen 2 was slightly weaker than specimen 1. In Specimen 3, the adhesive between the CLT and shear plates peeled off after passing 1/450, and the friction between the CLT and shear plates and the shear of the tensile bars resisted against horizontal force up to 1/300. Fracture of the tensile bars was confirmed after the horizontal displacement reached 120 mm. Finally, for specimen 4, the ultimate shear force of 62.0 kN, which is equivalent to the ultimate shear force of two shear bars, was reached at 1/450 of a cycle, but the shear force continued to increase after that because of the tensile rebars acting to resist not only tensile force but also shear force.

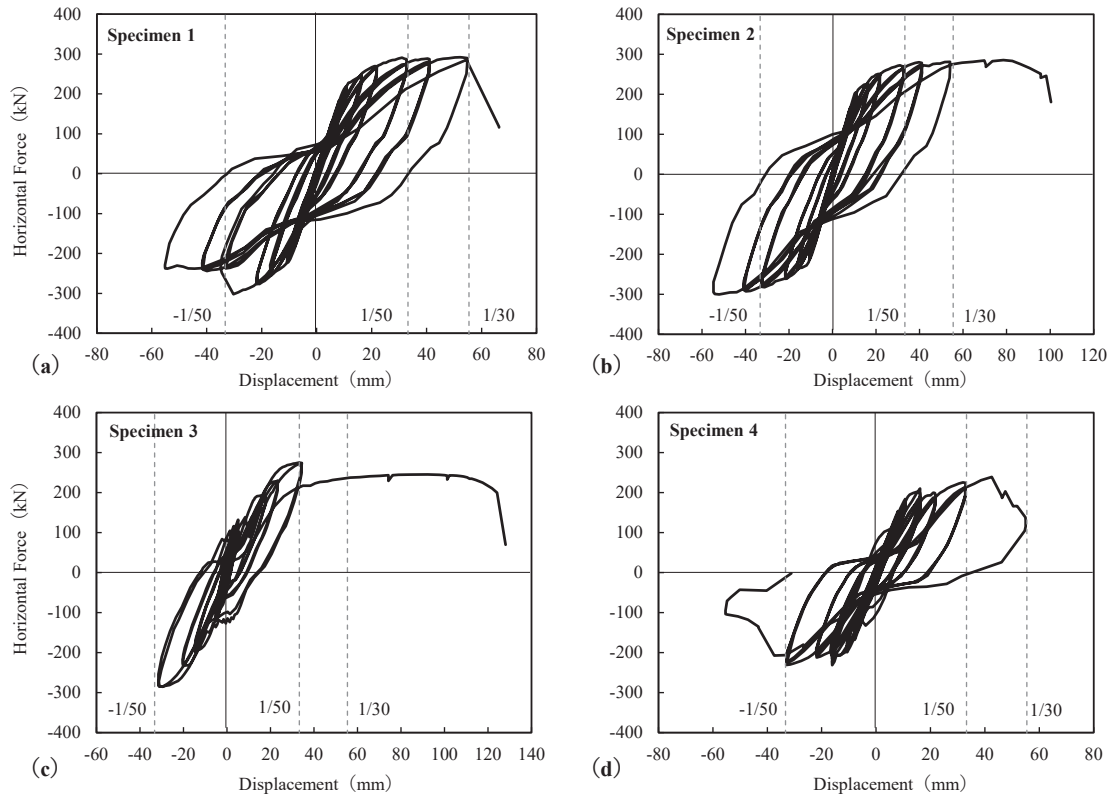

Figure 4: *Global response: (a) Specimen 1; (b) Specimen 2; (c) Specimen 3; (d) Specimen 4*

https://doi.org/10.52202/069179-0275

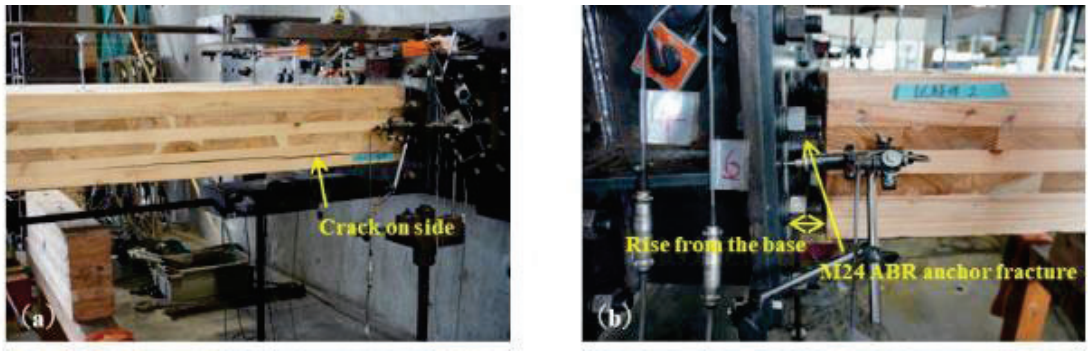

Figure 5: *Damage condition: (a) Specimen 1; (b) Specimen 2*

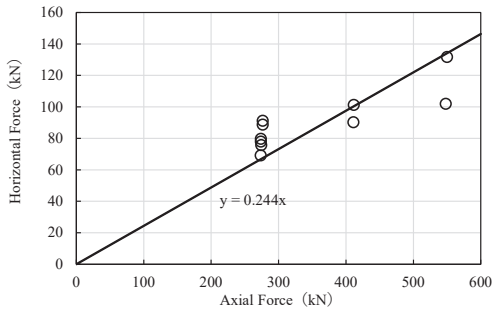

Figure 6: *Friction coefficient measured at specimen3*

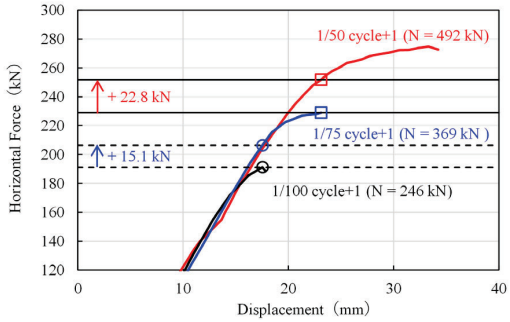

Figure 7: *Effect of axial force measured at specimen3*

The historical response of specimens 1 and 2, which were of the tensile bar pre-yielding type, was spindle-shaped, and energy absorption in the second and fourth quadrants was confirmed.

4.2 DAMAGE CONDITION

Figure 5 shows the damage of specimens 1 and 2. Specimen 1 had a crack on one side whereas specimen 2 had no damage. In the GIR joint with D22 rebar anchored 750 mm into the CLT, it was suggested that the CLT may have cracked and failed before the GIR exhibited its ultimate strength, because of the edge clearance distance. In the large deformation range, the separation between the CLT shear wall footing and the steel base increased, indicating that tensile forces were acting on the shear bars, which were expected to resist only shear forces.

4.3 FRICTION COEFFICIENT

Figure 6 shows the relationship between maximum horizontal and axial forces for each cycle measured on the positive side of the 1/450 and 1/300 cycles of specimen 3. The coefficient of static friction between the CLT and the steel base was calculated by the horizontal force divided by the axial force. The top flange of the steel base had a long hole along loading direction therefore the tensile bars didn't resist the shear force under such a small deformation range. The slope of the regression line (which means the static friction coefficient) was determined to be 0.244 using the least-squares method.

4.4 EFFECT OF AXIAL FORCE

Figure 7 shows the relationship between horizontal force and horizontal displacement for the first positive side up to 1/100, 1/75, and 1/50 for specimen 3. The horizontal forces increased by 15.1 kN by changing the axial force from 1.0 to 1.5 times during the transition from 1/100 to 1/75 cycles, and by 22.8 kN changing the axial force from 1.5 to 2.0 times during the transition from 1/75 to 1/50 cycles. The advantage of the self-centering ability: that the axial force snapped back to the initial position, was observed.

5 NUMERICAL ANALYSIS

5.1 NUMERICAL ANALYSIS MODEL

Hummel proposed a method for analysing the behaviour of CLT walls, which predicts the maximum strength and global response [7].

An attempt was made to reproduce the global response of specimen 2 using OpenSees, a general-purpose structural analysis framework [8]. Figure 7 shows an overview of the numerical analysis model, in which the CLT wall was represented by plastic beam-column elements and multi-springs were placed between the CLT wall footing surface, which was assumed to be rigid body, and the steel foundation. Tensile springs were placed at the same positions of the tensile and shear resisting bars, and a horizontal shear spring was placed in the center of the rigid body to consolidate the stiffness of the eight shear resisting bars.

https://doi.org/10.52202/069179-0275

Table 1 summarizes spring property of each spring. Detailed calculations are showed in the following section.

5.2 TENSILE SPRING PROPERTY OF TENSILE BARS

The elastic stiffness k_e of the tensile spring representing the tensile rebar and anchor was calculated from the following equation.

$$1/k_e = 1/k_{clt} + 1/k_a + 1/k_f \quad (1)$$

where k_{clt} = pull-out stiffness from GIR joint, k_a = tensile stiffness of ABR anchors, k_f = stiffness due to out-of-plane bending of the bottom flange

From previous studies [9,10], the tensile stiffness of the GIR joint with 750 mm anchorage length was 114 kN/mm, and the tensile stiffness of the D22 rebar exposed 300 mm length was 264 kN/mm. Pull-out stiffness from GIR joint was calculated by the series spring relationship.The tensile stiffness of ABR anchor was calculated from the axial stiffness with an effective length of 170 mm.

From the element tensile test of the M24 ABR anchor, the yield strength F_y, the ultimate strength F_u, the displacement of the yield shelf δ_1, and the secondary stiffness K_p were calculated. The stiffness after reaching the ultimate strength was set to zero. The yield strength in compression was set to 121 kN, which is the buckling strength following the Japanese code [11]. The effective buckling length l_b was set to 62.5 mm considering the stiffeners. Factors of safety were not considered when calculating the buckling strength in order to obtain a compression strength close to the actual behaviour. The stiffness after reaching the compressive yield strength was set to zero.

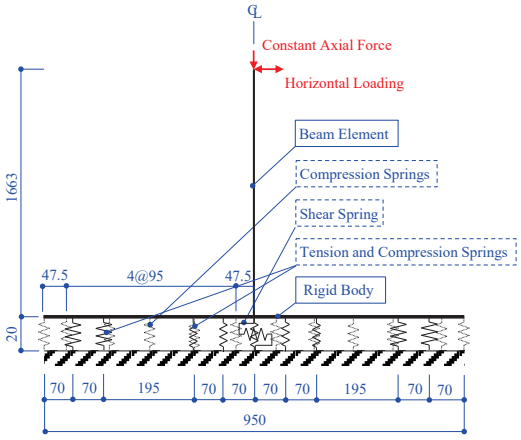

Figure 8: *Numerical analysis model*

5.3 TENSILE SPRING PROPERTY OF SHEAR RESISTING BARS

For the tensile stiffness of the shear resisting bars, a pullout stiffness of 54.5 kN/mm with an anchorage length of 210 mm was substituted for the tensile stiffness of the shear resisting bars from a previous study [12]. The shear resisting bars were assumed to resist only in tension since the effect of the shear resisting bars wasn't ignored in the large deformation range.

5.4 COMPRESSION SPRING PROPERTY OF CLT

The compression spring characteristics of CLT shear wall footing were calculated from the compressive stiffness and stress specified in the CLT-related Notification Manual and the Design and Construction Manual [12]. The effective width of the compression springs was set to 47.5 mm for the springs located at both ends of the rigid body, and 95 mm width for the other compression springs.

5.5 COMPARISION WITH TEST GLOBAL RESPONSE

Figure 9 compares the experimental and analytical global response of specimen 2. The analysis was in good agreement with the experiment results. The initial stiffness of the experimental and analytical results agreed at 19.1 kN/mm, and the maximum positive strength was 286 kN and 316 kN, respectively. The excursion to

Table 1: *Spring properties*

Type of springs	Tensile spring representing tensile resistance bar	Compression spring representing CLT wall	Tensile spring representing shear resistance bar	Shear spring representing shear resistance bar
Relationship between deformation and force	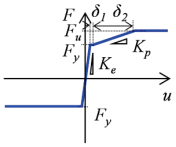	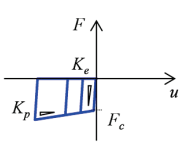	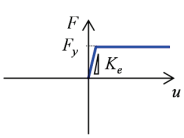	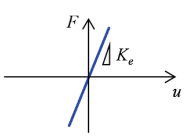
K_e Elastic Stiffness [kN/mm]	128	16.8 (edges) 33.7 (the others)	54.5	14.4
F_y Yielding strength [kN]	141(tension) 121(compression)	115 (edges) 230 (the others)	99.4	–
K_p Plastic Stiffness [kN/mm]	0.581	0.168 (edges) 0.337 (the others)	–	–
F_u Ultimate strength [kN]	201	–	–	–

https://doi.org/10.52202/069179-0275

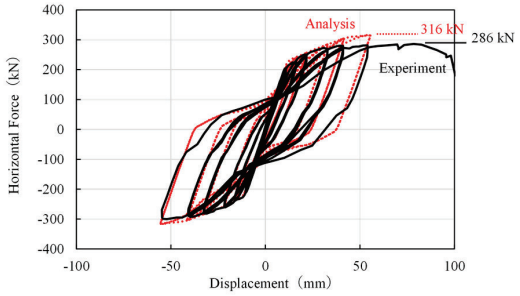

Figure 9: *Comparison experiment vs analysis*

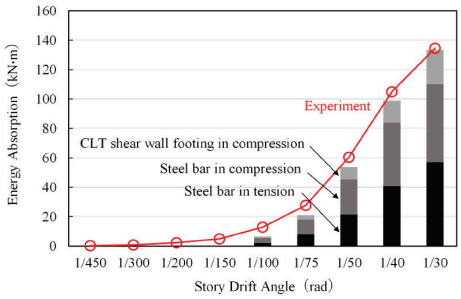

Figure 10: *Energy absorption*

unloading point from the peak strength, the experimental and analytical response showed slightly different behaviour. This difference is presumably due to the unloading stiffness of the tensile spring, that is set to be the same as the initial stiffness on the analysis, and there seems to be room for improvement in the modelling of the tensile spring.

5.6 ENERGY ABSORPTION

Figure 10 shows a comparison between experimental and analytical absorbed energy up to each cycle. The absorbed energy in the experiment is the sum of the horizontal displacement multiplied by the horizontal force at that point, i.e., the area bounded by the curve of the global response. The energy absorbed in the analysis was calculated from the response of tensile springs (simulating tensile resisting rebars) and compression springs (simulating the CLT wall footing). The energy absorption of tensile springs was defined as tension absorption when the axial force of the springs worked in tension and compression absorption was the opposite.

The larger the horizontal displacement, the better the agreement between the experimental and analytical values, with a difference of 3.37% at the 1/30 cycle. For the same cycle, the ratio of steel bars and CLT shear wall footing springs to the total energy absorption was 82.3% and 17.7%, respectively.

The energy absorbed by the steel bars on the compression side was 39.8% of the total energy absorbed, which means that the global response of the CLT shear wall exhibits a non-slip response.

6 CONCLUSION AND SUMMARY

Four CLT shear wall specimens with GIR joints were subjected to cyclic loading to examine the performance. A numerical model using OpenSees was developed to simulate the global response and confirm the energy absorption ability. Key results and observations are summarized below:

Specimens 1 and 2, which focused on using tensile rebars, exhibited great performance up to the 1/75 and exhibited a non-slip response because the M24 ABR steel anchors contributed to resisting in compression. In the GIR joint with D22 rebar anchored to the CLT by 750 mm, it was suggested that the CLT may crack and failed before the GIR exhibited its ultimate strength depending on the distance of edge.

The analysis model following Hummel proposed method reproduced the experimental behaviour of CLT shear wall specimen adequately. However, there was some room for improvement in the modelling of the tensile spring. The energy absorbed by the tensile resisting bars on the compression side was 39.8% of the total energy absorbed.

ACKNOWLEDGEMENTS

The authors are grateful to Yamasa Mokuzai Co.,Ltd., who contributed to making the test specimens and supported the experimental tests. The opinions expressed in this paper are those of the authors and do not necessarily reflect the views of individuals and organizations mentioned herein.

REFERENCES

[1] K. Kanazawa, H. Isoda, A. Kitamori, T. Usami, Y. Araki, Structural Performance OF Composite Structure WITH CLT Wall Infilled IN Steel Frames Using Drift-pin WITH Steel Plate, J. Struct. Constr. Eng., AIJ, Vol. 86, No.788, 1430-1439, Oct., 2021 (in Japanese)

[2] K. Morita, H. Umemori, T. Goshozono, M. Inayama, Development of medium-rise steel frame building with CLT shear wall. Part4 Horizontal load experiment of specimens with improved joint, Architectural Institution of Japan (AIJ) conference, Japan, 2020 (in Japanese)

[3] M. Kimura, S. Tsubata, O. Sadahiro, T. Kawachi, T. Hama, K. Kenji, Development of high strength shear wall using CLT (Part2 Structure experiment of high strength shear wall), Architectural Institution of Japan (AIJ) conference, Japan, 2017 (in Japanese)

[4] A. Mimatsu et al., Various Element Tests for the CLT Shear Wall using GIR Joints, Architectural Institution of Japan (AIJ) conference, Japan, 2018 (in Japanese)

[5] T. Carrero, J. Montañ, S. Berwart, H. S. María1, P. Guindos, Seismic behavior of innovative hybrid CLT-steel shear wall for mid-rise buildings, Bulletin of Earthquake Engineering (2021) 19:5917–5951

[6] I. Gavric, M. Fragiacomo, A. Ceccotti, Cyclic Behavior of CLT Wall Systems: Experimental Tests and Analysis Prediction Models, J. Struct. Eng., 2015, 141(11) 04015034.

[7] J. Hummel, Displacement-based seismic design

for multi-storey cross laminated timber buildings, Ph.D. Dissertation, Faculty of Civil and Environmental Engineering of the University of Kassel, Germany, 2017.
[8] McKenna, F., Object oriented finite element programming frameworks for analysis, algorithms and parallel computing. PhD thesis, University of California, Berkeley, California; 1997.
[9] S. Uesugi, D. Kadono, K. Murakami, Various Element Tests for the CLT Shear Wall using GIR Joints (Part2 GIR Joint Testing for the High Toughness Type CLT), Architectural Institution of Japan (AIJ) conference, Japan, 2021 (in Japanese).
[10] A. Mimatsu et al., Development and Construction of the Design Method of Two-way Flat Slab Using Cross Laminated Timber (Part2 GIR Joint Tensile Test and Shear Key Shear Test), Architectural Institution of Japan (AIJ) conference, Japan, 2019 (in Japanese)
[11] Architectural Institution of Japan (AIJ), Design Standard for Steel Structures -Based on Allowable Stress Concept-, Muruzen, Tokyo, Japan, 2019 (in Japanese)
[12] Japan Housing and Wood Technology Center, Design and Construction Manual for buildings using CLT, Japan, 2016 (in Japanese)

https://doi.org/10.52202/069179-0275